

VACUUM SYSTEM OF SPS-II: CHALLENGES OF CONVENTIONAL TECHNOLOGY IN THAILAND NEW GENERATION SYNCHROTRON LIGHT SOURCE*

T. Phimsen[†], S. Boonsuya, S. Chitthaisong, P. Sunwong, S. Prawanta, S. Chaichuay, K. Sittisard, T. Pulampong, S. Srichan, N. Juntong, P. Sudmuang, P. Klysubun
Synchrotron Light Research Institute, Nakhon Ratchasima, Thailand

Abstract

Siam Photon Source II (SPS-II) is Thailand's first 4th generation synchrotron light source. It not only provides high-energy and high-brightness synchrotron radiation for both academic and industrial research after its completion, but it also strategically aims to strengthen the Thai industrial community during the design and construction period. The vacuum system is expected to play a crucial role in enhancing the country's manufacturing capability. Most of the main components in the system are planned to be domestically fabricated through technology transfer. Instead of using NEG coating technology, the vacuum system design of the SPS-II storage ring is based on conventional technology, leveraging the potential and expertise of the Thai industry. This paper reviews the challenges and adaptations made in the traditional design of the dense DTBA magnet lattice, considering magnet aperture limitations. The vacuum chambers and bending magnets have been modified to accommodate IR beamlines, which are included in the second-phase plan. The pressure profile of the vacuum system in the storage ring is evaluated, and the progress of the overall vacuum system of SPS-II is described.

INTRODUCTION

Siam Photon Source II (SPS-II) is Thailand's first 4th generation synchrotron light source, currently under design and prototype development [1]. One of the key systems of SPS-II is the vacuum system, which is responsible for maintaining the high-vacuum environment required for the operation of the particle accelerators and beamlines. Most of the main components in the system are planned to be domestically fabricated through technology transfer. This domestic production of the SPS-II vacuum system presents a significant opportunity to enhance local manufacturing capabilities. It is worth noting that, in 2022, the manufacturing sector accounted for more than 27 % of Thailand's GDP, according to data from the World Bank [2].

Compact lattice designs, similar to MBA lattices found worldwide, present limited space for vacuum components. The small gap between magnet poles limits chamber conductance and makes it difficult to evacuate outgassing, primarily from photon stimulated desorption (PSD). Non-Evaporable Getter (NEG) coating technology has been adopted by many light sources to overcome this

limitation [3-5]. However, there are a few challenges associated with this technology that should be considered.

One issue to consider is the complexity of evenly and uniformly applying NEG coatings to intricate vacuum chambers. Complex geometries can make this application process challenging. Additionally, there is concern about the cost and complexity of replacing NEG coatings if they become contaminated or damaged, and the coatings' lifetimes.

Instead of relying on NEG coating technology, the vacuum system design for the SPS-II storage ring is based on conventional technology, harnessing the potential and expertise of the Thai industry. This strategic decision aims to strengthen the Thai industrial community during the design and construction phases.

After conducting parallel studies and development of prototypes for both SUS (stainless steel) and aluminum chambers, the decision to proceed with aluminum was made based on advice from RIKEN and NSRRC experts, as well as the constraints of a short research and development (R&D) period. The advantages of aluminum, including its lightweight nature, high strength-to-weight ratio, corrosion resistance, thermal conductivity, machinability, and cost-effectiveness, were key factors in selecting it as the material for further development.

VACUUM CHAMBER DESIGN

The lattice of the storage ring is the Double-Triple Bend Achromat (DTBA), which comprises 4 normal dipole magnets (BM), 2 combined-functions dipole magnets (DQ), 16 quadrupole magnets (QD, QF), 8 sextupole magnets, and 2 octupole magnets per cell as displayed in Fig. 1. The storage ring consists of 14 DTBA cells (23.393 m/cell), resulting in a total ring circumference of 327.502 m.

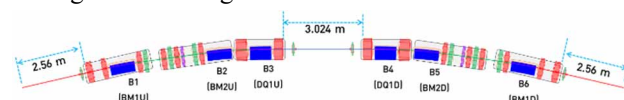


Figure 1: Schematic diagram of DTBA unit cell.

Each cell of the vacuum chamber can be divided into various sections: standard straight sections, middle straight sections, upstream arc section (including bending chambers PVCB-1 and PVCB-2), and downstream arc section (including bending chambers PVCB-3 and PVCB-4), as depicted in Fig. 2. The system has been designed to accommodate the use of three synchrotron radiation sources: two insertion devices (ID) located in the standard and middle straight sections, and the 5th bending magnet located in the downstream side of the cell.

* Work supported by Thailand's Science, Research, and Innovation Fund
[†] thanapong@slri.or.th

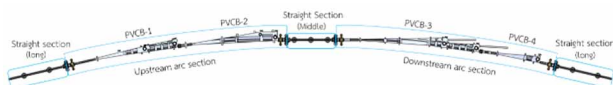


Figure 2: Schematic diagram of sectioned-vacuum chamber in DTBA unit cell.

Straight Section

Straight chamber will be manufactured using Al6063-T5 aluminum extrusion and will feature cooling channels along both sides. The cross-section of the beam duct will be elliptical in shape, with a vertical axis of 16 mm and a horizontal axis of 40 mm, matching the dimensions of the largest beam stay clear of the electron beam. This elliptical cross-section will be maintained consistently throughout the entire length of the beam duct. RF shield bellows will be installed on both side of the straight section to accommodate the thermal expansion during section baking-out (in the tunnel). The length measured from each yoke of the quadrupole magnets is 5.12 m for the standard straight section and 3.024 m for the middle straight section. However, these lengths need to accommodate the fast corrector chamber, BPM (Beam Position Monitor), gate-valve, and RF-shield bellow as well. As a result, the standard straight section or the middle straight section becomes shorter, limiting the available space for insertion devices. The available lengths of the standard straight section and middle straight section for insertion devices and relevant equipment are 4.1 m and 1.8 m, respectively.

Arc Section

Compared to NEG coated copper chamber, SPS-II bending chambers are very bulky. The chambers have been designed as triangular shape with long straight side of the chamber to be easier welded. Considering local manufacturing technology, the chamber has been designed as a two-different structure. It consists of straight parts made from Al6063-T5 aluminum extrusion and a Al6061-T6 bending part manufactured using CNC machining. The outside of the chamber will be machined to fit the shapes of poles and coils for the multipole magnets along the beam duct. Since the clearance between the chamber and the magnet is 1 mm typically, precise machining and positioning of the bending chamber are crucial to avoid any conflicts with nearby active components. The chambers have a minimum thickness of 1.6 mm due to the narrow space between magnet poles. To ensure sufficient structural strength, strategic thickening is applied to other sections outside the magnets, optimizing the overall thickness of the chamber. As a result, the maximum chamber's thickness, measured from top to bottom, is set at 80 mm.

Within the limited space between the magnets, photon absorbers and local pumps are strategically placed to take advantage of their effectiveness in localized pumping near the dominant PSD-outgas regime.

The entire upstream or downstream section will be baked in the laboratory before being transported and assembled in the tunnel. Consequently, a large RF-shield bellow is not required in this section. Instead, a single bellow will be installed between each chamber of each arc section to

minimize stress and accommodate thermal expansion during operation.

The structural simulations were conducted using ANSYS software. The simulations focused on analysing deformation and safety factors of structure. Parameter setting for simulation consists of forces due to chamber weight itself, photon absorbers weight, atmospheric pressure, the weight of the pump, a thermal condition of 35 °C, and earth gravity of 9.8106 m/s². The selection of fixed and sliding supports have been made with careful consideration to ensure that the simulation results yield stress and deformation within acceptable tolerances.

The simulation results for all bending chambers demonstrate acceptable values with longitudinal deformation of less than 1 mm, vertical and horizontal deformation of less than 0.3 mm. The structural simulation results of all chambers indicate that the stress and safety factor of the simulation are within acceptable tolerances. Figures 3 and 4, as examples, show simulation results of stress and vertical deformation of PVCB-1, respectively.

It is important to highlight that this design approach results in a notably large magnet, which is already an exceptionally thin structure due to the compact lattice configuration. As a result, vibration becomes a more significant concern.

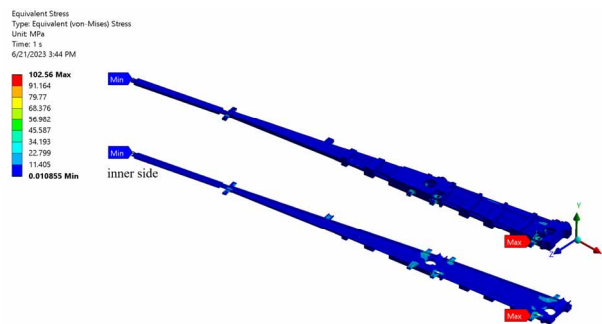


Figure 3: Stress of PVCB-1.

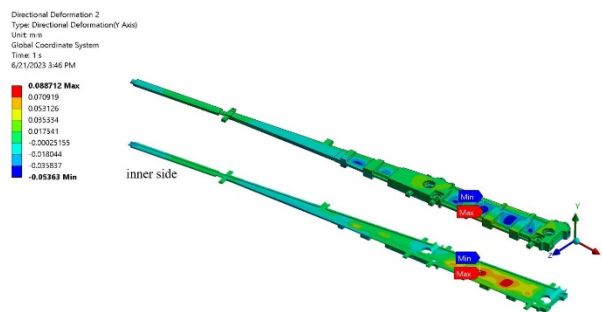


Figure 4: Vertical deformation of PVCB-1.

Bending Chamber for IR Extraction

Since Thailand is an agricultural country with biological diversity, an Infrared (IR) beamline is an important tool in this field of research. There is a plan to have two IR beamlines at SPS-II. However, due to concerns about beam instability and the complexity of designing IR extraction mirrors, the IR beamline has been placed as a second-phase project. Nevertheless, it is worth considering the design

Content from this work may be used under the terms of the CC-BY-4.0 licence (© 2023). Any distribution of this work must maintain attribution to the author(s), title of the work, publisher, and DOI

and exploring the possibilities, especially for magnet and vacuum chamber design, before it is too late.

IR requires a large vertical opening angle; therefore, it is necessary to modify the magnets and vacuum chamber to meet this requirement. The sixth bending magnet in the cell has been selected for use as an IR source. Considering the space and vacuum system design, this region is quite independent from the others, making it easier to replace. Bending magnet for IR extraction has been designed with a larger gap than an ordinary dipole but still uses the same operating current [6].

The cross-section of the chamber must be enlarged to accommodate the required opening angles of ± 20 mrad horizontally and ± 12.5 mrad vertically. Following this expansion, it should gradually taper down to the standard shape with taper of 1/8 before passing through the magnet. This taper may introduce higher impedance, which should be considered in the impedance budget and studied further for its potential impact on instability.

PHOTON ABSORBERS

Different types of OFHC copper photon absorbers have been designed to accommodate various heat loads and heating power densities. These absorbers can be categorized based on the shape of the copper groove: flat, V-shape fin, triangular fin, and rectangular fin as shown in Fig. 5. The flat and V-shape fin absorber has two cooling water pipes, while the triangular fin and rectangular fin absorbers have four cooling water pipes, divided into two upper pipes and two lower pipes.

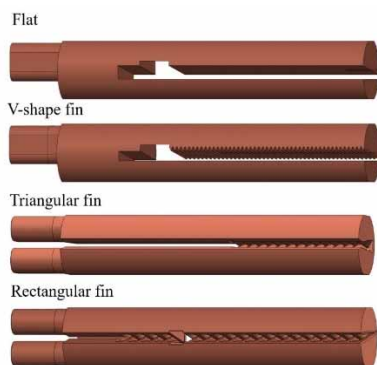


Figure 5: Type of OFHC copper photon absorber.

The simulations were conducted using ANSYS software by steady-state thermal and static structural modes. The simulations focused on analysing the deformation and safety factors of absorbers. For the simulation, the heat transfer coefficient (h) for the cooling water has been set to 10,000 W/mm². The ambient temperature and the inlet temperature of the cooling water are specified as 25 °C. Furthermore, the power of synchrotron radiation has been defined from the beam current of 600 mA which is two times higher than operation current target.

After conducting thermal and structural simulations on all seven OFHC absorbers, it has been determined that they

all meet the tolerances. Among them, ABS-B4 in PVCB-4 comes closest to the limits, with absorber and water temperatures of 145.31 °C and 91.879 °C, respectively. The stress and safety factor for ABS-B4 are 99.137 MPa and 2.371, respectively. Figure 6 displays the temperature distribution of absorber ABS-B4. Although the simulation results for ABS-B4 show maximum values approaching the specified criteria's boundary, they remain within the tolerance range for OFHC. This highlights one of the advantages of conventional chamber design, which reduces power density by positioning absorbers as far from the radiation sources as possible.



Figure 6: The temperature distribution of ABS-B4.

PRELIMINARY STUDY OF PRESSURE PROFILE

The one-dimensional iteration method is a powerful tool for calculating pressure profiles in the vacuum system of a synchrotron storage ring. It relies on three essential factors: pumping speed (S), outgassing rates (Q), and conductance (C). The outgassing rate (Q) is determined based on the photon flux and the PSD yield, which is conservatively estimated at approximately 10⁻⁶ molecules per photon at a dose of 100Ah for this specific analysis. The pressure profile is described by the equation:

$$S_i P_i = Q_i + C_i(P_{i-1} - P_i) + C_{i+1}(P_{i+1} - P_i). \quad (1)$$

In Eq. (1), "i-1," "i," and "i+1" represent the previous, current, and next mesh points in the system. This equation illustrates how the pressure at a specific point depends on various factors and the relationships between adjacent locations in the vacuum system, as shown in Fig. 7.

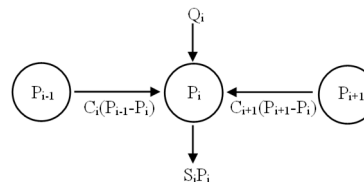


Figure 7: Layout of factors and the relationships between adjacent locations in calculation.

The conductance of a straight section is estimated to be 20 l/s, while bending chambers have a higher conductance of approximately 80 l/s. The calculation results show a very high average pressure of 4.66 x 10⁻⁹ mbar, which exceeds the tolerance. This is primarily due to limitations in conductance, as pressure profiles indicated in Fig. 8. High pressure is observed where there are no pumps especially at the beginning of the bending chamber.

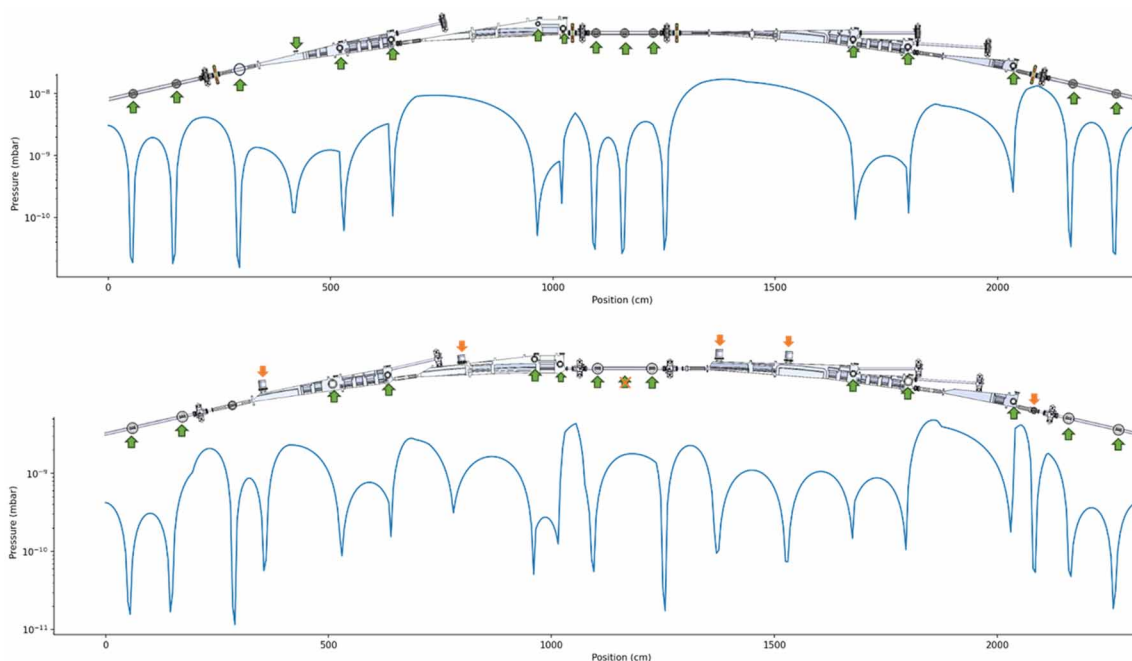


Figure 8: Pressure profile comparison of a single cell chamber between the original vacuum chamber design (top) and the improved design with additional pumps and conductance improvement (bottom). Green arrows indicate the location of the pumps along the cell, and the orange arrows indicate the additional pumps.

To address this, strategies for positioning photon absorbers and pumps to evacuate outgassing, primarily from PSD, have been explored. Additionally, the conductance of both bending chambers in the arc section and the dummy chamber in the straight section need to be improved. In this case, the antechamber size is increased, while the cross section of the dummy chamber in the straight section will be changed from an elliptical shape to a circular shape with an inner diameter of 40 mm. Figure 9 shows examples of improved cross-section design in the PVCB-4 case.

Figure 8 (bottom) shows an improved vacuum chamber layout featuring more pumps, resulting in an average pressure of 1.21×10^{-9} mbar, which is within tolerance. However, the structural and thermal properties of chambers and components need to be studied further, and the results should be confirmed using a Monte Carlo simulation program at the end. Besides, it is necessary to take an effort to reduce the dynamics outgassing as much as possible using oil-less machining technique and chemical cleaning.

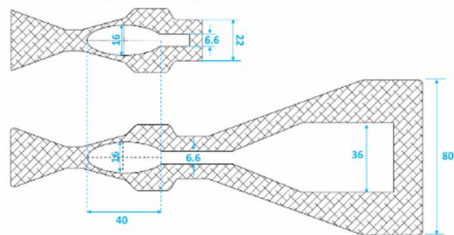


Figure 9: Comparison between cross section of bending chamber PVCB-4 before (top) and after (bottom) improving design.

DISCUSSION AND CONCLUSION

Conventional technology without NEG coating presents several challenges. First, finding adequate space for pumps, absorbers, and beam position monitors (BPMs) is very difficult. This can result in the sacrifice of straight section length, which in turn reduces the available space for insertion devices. Moreover, the bulky chambers require optimization of their thickness to achieve the best strength, necessitating more time and effort compared to using copper tubes. However, from the design perspective, the radiation synchrotron power density absorbed by absorbers is typically low. Therefore, photon absorbers made from oxygen-free high conductivity (OFHC) copper are sufficient to withstand the absorbed power.

The SPS-II project, which has received the Thai government's approval, will be situated within Rayong Province's Eastern Economic Corridor of Innovation (EECi). In line with Thailand's government development policy of fostering domestic manufacturing expertise, the project will prioritize local economic advantages by utilizing conventional vacuum technology.

Prototypes of vacuum chambers have been created to assess local manufacturing capabilities and pinpoint areas for improvement. High-precision machining, welding, and surface treatment techniques, such as oil-less machining and chemical cleaning, are the critical technologies that must be developed to meet the project's requirements. To prepare for the project, two welding technicians have received training, and a pilot plant has been constructed, which includes clean rooms for cleaning, welding, and assembly.

REFERENCES

- [1] P. Klysubun *et al.*, “SPS-II: A 4th Generation Synchrotron Light Source in Southeast Asia”, in *Proc. IPAC'22*, Bangkok, Thailand, Jun. 2022, pp. 764-768.
doi:10.18429/JACoW-IPAC2022-MO0PLGD2
- [2] <https://data.worldbank.org/country/thailand>
- [3] M. J. Grabski *et al.*, “NEG Thin Film Coating Development for the MAX IV Vacuum System”, in *Proc. IPAC'13*, Shanghai, China, May 2013, paper THPFI044, pp. 3385-3387.
- [4] R. M. Seraphim *et al.*, “Vacuum System Design for the Sirius Storage Ring”, in *Proc. IPAC'15*, Richmond, VA, USA, May 2015, pp. 2744-2746.
doi:10.18429/JACoW-IPAC2015-WEPMA003
- [5] C. Herbeaux, N. Béchu, and J.-M. Filhol, “Vacuum Conditioning of the SOLEIL Storage Ring with Extensive Use of NEG Coating”, in *Proc. EPAC'08*, Genoa, Italy, Jun. 2008, paper THPP142, pp. 3696-3698.
- [6] P. Sunwong *et al.*, “Design of dipole magnets for Siam Photon Source II”, *J. Phys. Conf. Ser.*, vol. 2431, p. 012072, 2022. doi: 10.1088/1742-6596/2431/1/012072